

# Single crystal microwave dielectrics at low temperature: losses and non-linearities

John Gallop\*, Ling Hao

*National Physical Laboratory, Queens Road, Teddington TW11 0LW, UK*

## Abstract

Single crystal dielectrics (SCDs) at cryogenic temperatures ( $< 100$  K) provide some of the highest  $Q$  microwave resonators which may be realised and, as a result, may have important applications across the microwave communications industry. We summarise measurement techniques used for characterising the complex permittivity of single crystal dielectrics at cryogenic temperatures. Various measurement geometries are described, including Courtney resonators, composite dielectric pucks, an indirectly heated high  $Q$  resonator perturbation technique (using both microwave and bolometric readouts) and coupled dielectric resonators. A potential technique for making spatially resolved measurements on a scale small compared with the free space wavelength is also outlined. The methods are illustrated by measurements made on a range of single crystal materials including sapphire, rutile and strontium titanate. Numerical modelling is an important element in accurate evaluation of the measurement data and this will also be considered. Until now the thermal properties of the dielectrics have been ignored in evaluating their microwave properties. We suggest that this is an issue which should not be neglected, particularly when considering the non-linear behaviour of the permittivity as a function of microwave power.

© 2003 Elsevier Ltd. All rights reserved.

*Keywords:* Low temperature; Microwave dielectric properties; Oxides

## 1. Introduction

Single crystal dielectrics (SCDs) at cryogenic temperatures ( $< 100$  K) provide some of the highest  $Q$  microwave resonators which may be realised and, as a result, may have important applications across the microwave communications industry. The (somewhat delayed) introduction of 3G/UMTS systems puts pressure on available bandwidth (broad-band multi-media and data as well as voice). Base-station filters in both transmit and receive paths must have steeper walls to avoid cross-talk since UMTS does not allow for guard bands between its 5 MHz wide channels. A likely result is an accelerated adoption of cryo-cooled base stations (at present  $> 1500$  cryo-base stations are installed or ordered in the USA, doubling every year, and the Japanese market seems set for rapid expansion). To achieve steep sided filter walls in a multipole filter each element must have as high a  $Q$  value as possible. Two cryo-cooled technologies are competing at present to provide the highest  $Q$  microwave resonators: (1) high

temperature superconductor (HTS) oxide thin film circuits and (2) single crystal oxide dielectric resonators (such as  $\text{Al}_2\text{O}_3$ ,  $\text{LaAlO}_3$  ...). A crucial issue involves non-linear properties within the filters and we point out below that dielectric materials also exhibit non-linearities at high powers, an aspect of their behaviour which is often ignored.

## 2. Properties of single crystals at cryogenic temperatures

Many properties of single crystal materials show general improvements when their temperature is reduced below ambient temperature, especially the loss tangent and the temperature coefficient of the real component of the permittivity. SCDs have generally lower losses than polycrystalline or amorphous dielectrics at room temperature but this difference is exaggerated as the temperature  $T$  falls.<sup>1</sup> For simple ionic materials, with strongly directional covalent bonds and low dislocation densities, such as the single crystal oxides which are widely used as dielectric materials at microwave frequencies, intrinsic loss mechanisms arising from the

\* Corresponding author. Fax: +44-20-8943-6939.  
E-mail address: [john.gallop@npl.co.uk](mailto:john.gallop@npl.co.uk) (J. Gallop).

anharmonic component of the interionic potential, are strongly reduced as  $T$  falls. Fig. 1a shows results measured in the author's lab of the permittivity of sapphire a function of temperature. Sapphire,  $\text{Al}_2\text{O}_3$  has a hexagonal structure and consequently the  $c$  axis permittivity is different from that measured for the  $a$ – $b$  plane by some 20%. The observed losses in sapphire (see Fig. 1b) fall with an approximately  $T^5$  dependence, reflecting the

change of the unit cell size, until extrinsic losses begin to dominate.<sup>2</sup> The very low loss-tangent for sapphire observed at cryogenic temperatures (as low as  $3.10^{-10}$  at 1.5 K and 3 GHz) has led to at least two different application areas, both exploited first by the group at the University of Western Australia. First as the read-out resonator for a highly sensitive displacement detector for a resonant bar gravity wave antenna<sup>3</sup> and more recently as the state-of-the-art flywheel oscillator which complements the long-term stability of a cold-atom fountain frequency standard by providing exceptionally low phase-noise for shorter averaging times.<sup>4</sup> Loaded  $Q$  values as high as  $5 \times 10^9$  have been exploited in this latter application.

Titanium dioxide ( $\text{TiO}_2$ , rutile) has a considerably higher permittivity than sapphire, between 210 and 80 at room temperature, depending on the crystal axis along which  $\epsilon_r$  is measured. It possesses two important attributes: the loss tangent is only a small factor greater than that of sapphire, at least down to around 50 K and it has the opposite sign for the temperature coefficient  $d\epsilon_r/dT$ .<sup>5</sup> A third general class of dielectrics has extremely high  $\epsilon_r$  at all temperatures and may enter an ordered, ferroelectric phase as  $T$  falls. Thus for example, strontium titanate ( $\text{SrTiO}_3$ ) is a perovskite-structured insulator with an exceptionally high relative permittivity. At low temperatures it enters a paraelectric state before becoming a ferroelectric below about 35 K.

### 3. Measurement methods

The dominant measurement methods are based on resonant structures. These have the disadvantage that they are essentially narrow-band but a huge advantage that the sensitivity attainable for measurement of both real and imaginary components of the permittivity is much higher than that of any broadband technique. Since losses in SCDs are generally much lower than those exhibited by polycrystalline or amorphous samples this is an important consideration. Here we describe briefly a number of resonator techniques, each with its own advantages and limitations.

#### 3.1. Bare dielectric resonator

A high-symmetry shaped specimen of SCD in free space will exhibit standing wave resonances whose frequencies depend on the dimensions of the resonator and the permittivity  $\epsilon_r = \epsilon_1 + j\epsilon_2$ . If  $\epsilon_r \gg 1$  the standing wave field pattern is strongly confined within the dielectric itself. To a reasonable approximation the field distributions for each eigenmode (frequency  $f$ ) can be calculated for a highly symmetrical piece such as a rectangular parallelepiped or a right circular cylinder. Then, having measured the principal dimensions of the

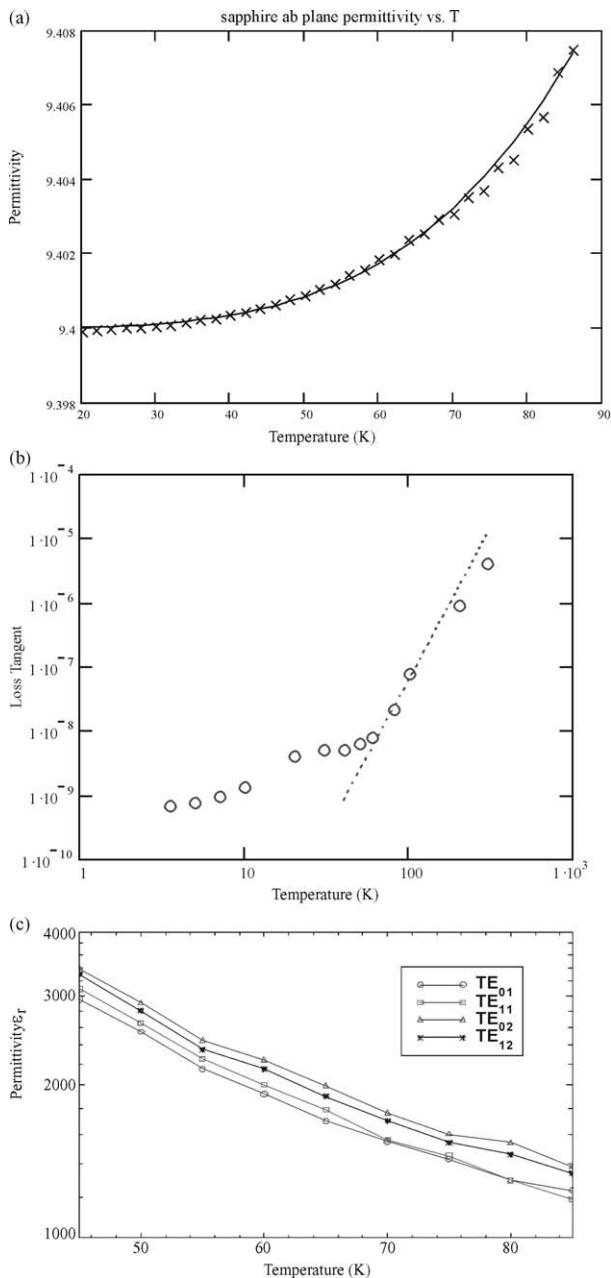


Fig. 1. (a) Temperature dependent permittivity  $\epsilon_r$  for  $\text{Al}_2\text{O}_3$ . (b) Temperature dependence of loss tangent of sapphire (see Ref. 2). The dashed line is a fit of the higher temperature data to a  $T^{4.75}$  power dependence. (c) Temperature dependent permittivity  $\epsilon_r$  for  $\text{SrTiO}_3$  substrate ( $10 \times 10 \times 0.5 \text{ mm}^3$ ), metallised top and bottom, measured using a parallel plate geometry.

resonator the real part of the permittivity can be calculated. Measurement of the unloaded resonant mode linewidth  $\Delta W$  then allows  $\varepsilon_2$  to be deduced, from the relationship [Eq. (1)]

$$\varepsilon_2 = \frac{\varepsilon_1 \Delta W p_e}{f} \quad (1)$$

where  $p_e$  is the electric filling, provided the entire loss can be assigned to the dielectric sample. In practice there is, inevitably, a finite electromagnetic field amplitude outside the dielectric and, since this is free space, power can be radiated away to infinity. This is an additional loss mechanism which therefore limits the accuracy of the determination of  $\varepsilon_2$ . In addition the resonator frequency may be perturbed by objects existing in the far field region, well away from the dielectric itself.

### 3.2. Dielectric resonator enclosed in a metallic housing

Both of these problems can be much alleviated by enclosing the dielectric in a tight fitting enclosure, such as a metallic box. If this is a tightly fitting enclosure the eigenmodes are the same as those of a cavity resonator of the same size, suitably scaled by  $(\varepsilon_r)^{-1/2}$ . It is of course essential that the inevitable losses arising at the enclosing walls should be much less than the loss in the dielectric. For very low loss dielectrics this is difficult to arrange and has led to the use of superconducting enclosures, such as either the conventional metallic superconductors (for measurements made with  $T < 15$  K) or the newer cuprate superconductors which can be produced with very low microwave losses even at temperatures up to 100 K.

### 3.3. Parallel-plate resonator

A fully enclosed dielectric sample is challenging to prepare. It turns out that for samples of thickness  $t$  such as discs or rectangular solids (where  $t < \lambda_d$ , the wavelength of the standing wave pattern within the dielectric at the measurement frequency  $f$ ) a good approximation to a full enclosing conducting surface can be achieved by sandwiching the dielectric plate between two equally sized copper (or superconducting) plates. Then the corrections due to finite field penetration beyond the unclad edge of the sandwich can be neglected in most situations.

### 3.4. Courtney resonator

A modification of the parallel plate resonator, known as the Courtney resonator geometry, is much used for room temperature measurements. This consists of a dielectric puck, sandwiched between two end plates made of a good conductor, but with radius  $r_C$  much

greater than that of the puck, which serves to further limit the edge-radiating losses. The larger end plates can be used for a variety of dielectric radii  $r_d$  provided the inequality  $r_d < r_C$  is not compromised. The Courtney geometry can be used at cryogenic temperatures but for very low loss dielectrics such as sapphire the conductor loss in this geometry cannot be neglected and will generally exceed the dielectric contribution.

### 3.5. Whispering gallery modes

Some dielectrics such as sapphire at low temperature have such low losses that even this approach cannot produce a housing with negligible losses compared with that of the dielectric. In this case, rather than using a low order resonant mode (such as the  $TE_{011}$  mode for a cylindrical geometry, which typically has the highest  $Q$ ), so called whispering gallery modes are employed, which have a large number of nodes around the circumference. These confine the standing wave pattern more effectively within the dielectric than do low order modes. If the metallic housing is now spaced away from the dielectric (using low loss dielectric support elements to rigidly maintain the axial spacing of the single crystal sample) the evanescent field outside the dielectric decays exponentially rapidly so the losses on the metallic enclosure may be made negligibly small.

### 3.6. Bolometric techniques

All of the methods dealt with so far are concerned with perturbations to a high  $Q$  resonator mode, arising from temperature dependent changes to  $\varepsilon_1$  and  $\varepsilon_2$ . In the following section we estimate some limits to this detection sensitivity. There is an entirely different approach which may be followed with the highest quality single crystals, to measure at least the imaginary component of the permittivity with potentially higher sensitivity than any of the perturbation techniques. This is a bolometric method in which the temperature rise produced in the dielectric by absorbed microwave power is measured. Generally the thermometer must be kept outside the resonator enclosure since almost all thermometers involve lossy materials which would compromise the measurement accuracy. The most straightforward technique attaches an external thermometer to the SCD using a rod of low-loss single crystal sapphire. This material combines the lowest microwave loss with one of the highest thermal conductivity. The general idea is illustrated in Fig. 2. In the situation that the sample under measurement has already had  $\varepsilon_1(T)$  determined over the range of interest the puck may be used as its own thermometer, provided the thermal conductance of its links through the support structure and thence to the constant temperature thermal bath may also be determined.

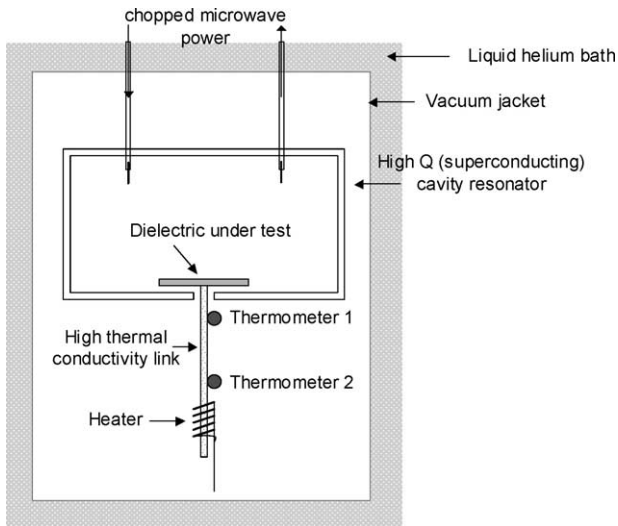


Fig. 2. Schematic of SCD sample enclosed in high  $Q$  superconducting cavity resonator with external temperature measurement for bolometric detection of losses.

Both of these bolometric methods are generally used in a pulsed mode. Thus the microwave power input to the resonator is chopped periodically. The temperature of the puck  $T_p(t)$  is monitored as a function of time and its time dependent temperature following the end of the pulse allows the thermal time constant  $\tau$  of the puck to be determined since it is this constant which determines the relaxation rate of the puck temperature towards the stable bath temperature of the resonator housing.  $\tau$  is simply related to the heat capacity of the puck  $C_p(T)$  and the thermal conductance  $G(T)$  of the support structure [see Eq. (2)], assuming that the thermal conductivity of the single crystal puck is great enough that it always comes to a uniform temperature in a time short compared with  $\tau$ .

$$\tau = \frac{C_p(T)}{G(T)} \quad (2)$$

### 3.7. Spatially resolved methods

An increasingly important issue involves the quality control of low-loss dielectric single crystals for microwave applications. Particularly for the higher permittivity materials and those involved in ferroelectric applications the losses can vary quite dramatically from sample to sample, and even within a single sample. The resonator methods outlined in this section have been modified to allow very localised measurement of the loss tangent within a dielectric material which may then be analysed by scanning the resonator over the surface of the dielectric sample under examination.<sup>6,7</sup> The NPL

developed method<sup>6</sup> employs a dielectric puck system which can be moved over the surface of a large dielectric wafer, sampling the permittivity at a number of discrete frequencies between 5 and 15 GHz. The permittivity can also be rapidly measured as a function of microwave electric field strength. Spatial resolution for the prototype system using a rutile puck is as small as 1–2 mm. The real and imaginary components of  $\epsilon_r$  can be measured by using a loop oscillator which can be interrupted by a fast microwave switch. The decay of microwave power in the resonator is then monitored as a function of time to determine the power dependent loss tangent. This process is extremely fast and straightforward and the loop oscillator configuration permits only relatively inexpensive components to be used. A group at the University of Maryland have taken this to a much higher level of spatial resolution by using a length of coaxial transmission line as a resonator,<sup>7</sup> which has an open end with a sharpened centre conductor. This tip is brought close to the dielectric sample to be sampled and scanned over the surface. Again the change in  $Q$  and frequency of the resonator allow spatial variation of  $\epsilon_r$  to be deduced. This system is particularly suited to scanning high permittivity dielectrics and spatial resolution down to a few microns has been achieved.

## 4. Modelling

For all of the measurement methods outlined above it is necessary to be able to accurately relate the stored microwave energy within the dielectric puck, compared with the input and output power from the resonator. For the case of the simplest, high symmetry geometries and for isotropic permittivities this may be done by analytical solution of the wave equation (for example, for an isotropic dielectric cylinder entirely enclosed in a high conductivity box, with no air gap between box and dielectric puck.) But for the more general cases one must resort to approximate mathematical methods to achieve satisfactorily accurate solutions. At least three different generic approaches are in fairly wide use: mode matching methods, the Rayleigh-Ritz variational method<sup>8</sup> and finite element techniques. A number of commercially available software packages allow the solution of Maxwell's equation for the interior of a generalised resonator structure consisting of anisotropic dielectric or magnetic materials, and lossy conductors. Each technique has its own advantages and disadvantages. The availability of ever-faster personal computers means that the finite element models which were previously expensive computationally compared with other methods are now gaining in popularity, especially since they are applicable to more complex geometries than the other methods.

## 5. Applications

We have already noted the commercial importance of cryo-cooled dielectric resonators to the future microwave communications industry. Below we describe just two somewhat esoteric applications of low loss SCDs, to indicate the possible breadth of future applications.

### 5.1. Coupled dielectric resonators

The authors are currently working on a novel form of bolometer, based on coupled microwave resonators, which may have widespread application in fields requiring sensitive measurement of the energy absorbed by the impact of particles, whether they be massive particles, photons or even phonons. The detector has emerged from work on functional oxide materials carried out over recent years.<sup>9</sup> The basic idea rests on a system of two coupled microwave resonators, one of which acts as a stable reference frequency but the other of which has a strong temperature dependent frequency [in the present prototype this is made of SrTiO<sub>3</sub> (STO) which has a very strong temperature dependence of its permittivity  $\epsilon_r$ ].<sup>10</sup> A key property of this resonator is that if the correct mode is chosen the frequency shift of the coupled mode with temperature does not depend on the volume of the temperature dependent resonator, at least to first order. Thus when energy is absorbed by the STO resonator its temperature changes, resulting in a frequency shift in the coupled resonance. Since extremely small frequency shifts are relatively easily detected this temperature sensor can have nK sensitivity. It also possesses other potential advantages over other sensors types. It is essentially non-contacting, in that interrogation of the temperature is done by the microwave field itself, no cables are required to contact the sensor. Secondly the sensor is an insulator. Its thermal capacity is due only to phonon contributions and there is no electronic contribution. At temperatures below 1 K the electronic contribution to the specific heat of metals far outweighs the lattice contribution. Thus an insulating sensor of a particular mass can have a much smaller heat capacity than a metal of similar mass at the same temperature so it may have higher resolution than a metallic one or could be operated at a higher temperature with the same resolution.

As an example consider the situation when the microwave fields of a sapphire and STO puck (within the same housing) are only extremely weakly coupled. Then the resonant frequency of a particular mode of the sapphire puck  $f_0$  (assumed temperature independent to a first approximation) is quite unaffected by the STO except for a temperature selected resonance condition when the resonant frequency  $g_0(T)$  of a mode in the STO comes into close coincidence with that of the selected sapphire mode. In this situation there is a

measurable interaction between the two modes so that they may be treated as coupled independent resonators.<sup>11</sup> The true time independent eigenfunctions are now represented as symmetric and antisymmetric linear combinations of the two unperturbed eigenfunctions. However, within the limits of perturbation theory the following four Eqs. (3.1)–(3.4) describe the resulting temperature dependent frequencies  $f(T)$  and  $g(T)$  and linewidths  $W_{\text{sap}}(T)$  and  $W_{\text{STO}}(T)$  of the observed coupled resonances:

$$f(T) = f_0 + \text{Re} \left[ \frac{A}{(f_0 - g(T)) + iW_{\text{STO}}} \right] \quad (3.1)$$

$$g(T) = g_0(T) + \text{Re} \left[ \frac{A}{(g_0(T) - f_0) + iW_{\text{sap}}} \right] \quad (3.2)$$

$$W_{\text{sap}}(T) = W_{\text{sap}} + \text{Im} \left[ \frac{A}{(f_0 - g(T)) + iW_{\text{STO}}} \right] \quad (3.3)$$

$$W_{\text{STO}}(T) = W_{\text{STO}} + \text{Im} \left[ \frac{A}{(g_0(T) - f_0) + iW_{\text{sap}}} \right] \quad (3.4)$$

Here  $A$ ,  $B$  are the normalised coupling strengths between the two modes, proportional to the overlap of the electromagnetic standing wave patterns of the stored energy of the two field distributions of the modes, integrated throughout the housing.  $W_{\text{sap}}$  and  $W_{\text{STO}}$  are the unperturbed linewidths of the sapphire and STO resonances, respectively. Which of the two coupled modes is observed in any experiment depends on the nature of the input and output coupling structures, especially their positions. If these are situated closer to the sapphire puck then the mode observed is the one which has the dominant stored energy within the sapphire puck. Explicit forms for the coupling coefficients  $A$  and  $B$  [Eqs. (4) and (5), respectively] may be written as follows:

$$A = \frac{f_0^2 \int_{\text{vol}} E_{\text{sap}} \cdot E_{\text{STO}} d\tau}{\int_{\text{vol}} E_{\text{sap}}^2 d\tau} \quad (4)$$

$$B = \frac{g^2(T) \int_{\text{vol}} E_{\text{sap}} \cdot E_{\text{STO}} d\tau}{\int_{\text{vol}} E_{\text{STO}}^2 d\tau} \quad (5)$$

where  $E_{\text{sap}}$  and  $E_{\text{STO}}$  are the electric field vectors for the relevant modes in sapphire and STO respectively. We can differentiate the first of our coupled resonator equations to determine how to maximise the response of  $f(T)$  to a change in STO temperature. It is simply shown that the maximum sensitivity to frequency occurs when the resonances of STO and sapphire exactly coincide when

$$\left. \frac{df(T)}{dT} \right|_{\max} = \left[ \frac{A}{(W_{\text{STO}})^2} \frac{dg(T)}{dT} \right] \quad (6)$$

The first term on the right of Eq. (6) is the ‘amplification factor’ by which the sensitivity of the coupled system is enhanced over the frequency variation with  $T$  of the frequency of the STO resonator alone  $[dg(T)/dT]$ . Thus it is important to operate with coupling between the resonators which is as strong as possible, with the loss tangent ( $\tan\delta$ ) of the STO as low as possible (to minimise  $W_{\text{STO}}$ ).

To demonstrate the potential of the coupled resonator method we have used STO and sapphire pucks (12 mm diameter) spaced by  $\sim 8$  mm in the axial direction. The resonant frequency of the  $\text{TE}_{011}$  mode in the sapphire puck has been measured as a function of temperature over a wide range (from 20 to 80 K). Fig. 3 illustrates how the frequency and linewidth of a sapphire resonance changes with temperature as two separate resonances in the STO component come successively into co-incidence with the sapphire mode. We have reported elsewhere<sup>12</sup> that the variation of both frequency and width of a coupled resonance can be quantitatively fitted by the above equations and that the rate of change of resonant frequency with temperature  $df(T)/dT$  can be as high as 75 MHz/K. Since the output frequency of a microwave loop oscillator based on a modestly high Q dielectric resonator can be stable to at least 1 in  $10^{11}$  for an averaging time of 1 s<sup>13</sup> the thermometer has a potential resolution of at least 1.5 nK, comparable with low temperature superconducting transition edge thermometers but operating a factor of 10 higher in temperature. The latter would be required to be separately temperature compensated using, for example a combination of sapphire and rutile elements,<sup>14</sup> as described in the following section.

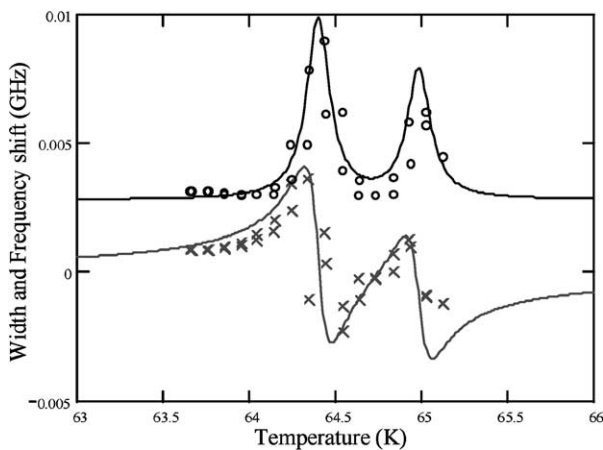


Fig. 3. Experimental results for the temperature variation of a coupled mode (predominantly the  $\text{TE}_{011}$  mode in sapphire) as the temperature is changed over a small range. The solid curves represent fits to the experimental data for frequency shift (bottom) and linewidth (top).

## 5.2. Microwave frequency standard based on a composite dielectric resonator

The principle of using a composite dielectric resonator composed of at least two different low loss dielectrics with opposite signs for the temperature dependence of their permittivities has been shown to allow high frequency stability with only moderate temperature control requirements.<sup>12</sup> The long-term aim of this work is to build an oscillator based on a whispering gallery (WG) mode resonance in such a composite resonator with a fractional frequency stability of better than  $10^{-13} \tau^{-1/2}$ , suitable as a flywheel standard for Cs primary clocks. The construction of the composite resonator is as follows: a stack consisting of a quartz disc (radius = 10.5 mm and height = 12 mm), a thin (radius = 10.5 mm and height = 0.4 mm), rutile disk and a sapphire puck (radius = 16 mm and height = 15 mm), enclosed in a cylindrical housing machined from OFHC-copper (Fig. 4). The ratio of stored energy in the rutile component, compared with that in sapphire, is the filling factor  $\kappa$  which determines the frequency  $f$  versus temperature  $T$  behaviour of the resonator and the turning point temperature  $T^*$ , at which  $df/dT=0$ . In order to achieve the required value of  $\kappa$ , and thus of  $T^*$ , with a rutile plate thickness  $> 100 \mu\text{m}$  (required for robustness) the diameter of the plate has to be smaller than the diameter of the sapphire disk. The plate diameter was optimised with respect to azimuthal mode number of the WG mode ( $7 < n < 12$ ) using MAFIA software. Note that the original dimensions were chosen to yield a whispering gallery mode at or close to the Cs hyperfine frequency (since an anticipated application of this device is as an ultra-low phase noise flywheel oscillator in support of Cs fountain or beam standards). In practice the

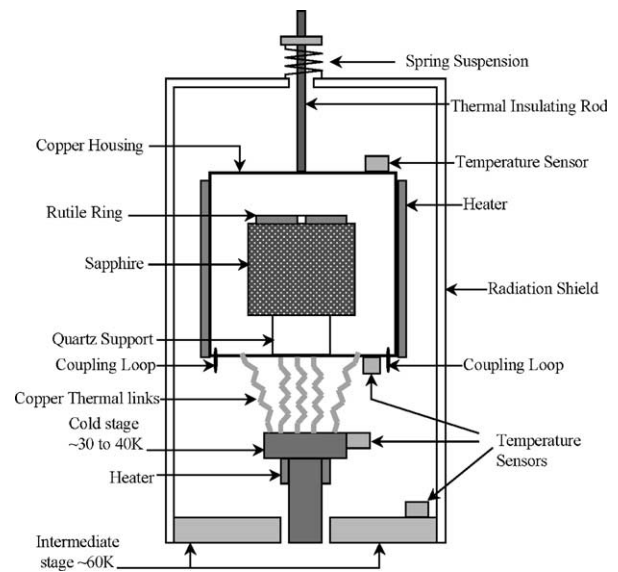


Fig. 4. Schematic of resonator construction, showing details of measures for cooler vibration isolation.

Table 1  
Summary of some properties of SCD materials

Material	Crystal structure	$\epsilon_1$ (300 K)	$\epsilon_1$ (70 K)	$\epsilon_2$ (300 K)	$\epsilon_2$ (70 K)	$\kappa$ 100 K W/m, K
Al <sub>2</sub> O <sub>3</sub>	Trigonal	11.5 ( <i>c</i> axis) 9.4 ( <i>ab</i> plane)	11.3 ( <i>c</i> axis) 9.3 ( <i>ab</i> plane)	$5 \times 10^{-6}$	$6 \times 10^{-9}$	300
MgO	Cubic	9.8	9.72	$1 \times 10^{-5}$	$2.5 \times 10^{-6}$	300
LaAlO <sub>3</sub>	Rhombohedral	24.0	23.4	$2 \times 10^{-5}$	$4 \times 10^{-6}$	20
TiO <sub>2</sub>	Tetragonal	170 ( <i>c</i> axis) 85 ( <i>ab</i> plane)	240 ( <i>c</i> axis) 105 ( <i>ab</i> plane)	$8 \times 10^{-5}$	$1.7 \times 10^{-6}$	–
SrTiO <sub>3</sub>	Cubic	350	$1.2 \times 10^3$	$2 \times 10^{-3}$	$2 \times 10^{-4}$	–

Values are indicative and represent average values from various published data.

frequency of the selected mode is 9.2984 GHz, with a difference between model and experimental frequency which amounts to  $\sim 1\%$  in this case. We have demonstrated with other designs that agreement should be attainable at least to a factor of 10 greater than this. These calculations show that the loss contributions from the quartz support and copper shielding cavity may be made negligible by suitable choice of dimensions.

## 6. Future directions and requirements

This paper has reviewed some of the unique properties exhibited by SCD materials at microwave frequencies and cryogenic temperatures Table 1. It is clear that these materials promise much for future applications, both in terms of commerce and science. There remains much which is not yet clearly understood and here a key issue is the nature of microwave loss mechanisms in imperfect single crystals. If these mechanisms could be better understood and thereby reduced, the importance of this class of materials would be much increased.

All of the materials discussed here are rather simple oxides but many future important applications areas may be expected from measurements on, and an understanding of, much more complex materials containing multiple cationic species. Advances in materials modelling techniques may allow specific properties such as permittivity to be designed from the bottom up and such a capability would also greatly increase the future utility of microwave dielectrics.

Microwave dielectrics are already sufficiently pure and defect free that they approach the loss tangent values associated with intrinsic processes. Cryogenic operation will remain an important route for enhanced low-loss performance. We can expect considerably simplified cryogenic temperature production and maintenance over the coming years, associated with the wide spread use of closed-cycle coolers. The development of reliable and relatively cheap coolers has already progressed rapidly as a result of wider use of superconductors and further improvements are to be expected.

## References

1. Krupka, J., Geyer, R. G., Kuhn, M. and Hinken, J. H., Dielectric properties of single crystals of Al<sub>2</sub>O<sub>3</sub>, LaAlO<sub>3</sub>, NdGaO<sub>3</sub>, SrTiO<sub>3</sub> and MgO at cryogenic temperatures. *IEEE Trans MTT*, 1994, **42**, 1886–1889.
2. Braginsky, V. B., Ilchenko, V. S. and Bagdassarov, K. S., Experimental observation of fundamental microwave absorption in high-quality dielectric crystals. *Phys. Lett. A*, 1987, **120**, 300–305.
3. Cuthbertson, B. D., Tobar, M. E., Ivanov, E. N. and Blair, D. G., An ultra-high quality factor microwave sapphire loaded superconducting cavity transducer. *IEEE MTT S International Microwave Symposium Digest*, 1996, **3**, 1489–1492.
4. Krupka, J., Cros, D., Luiten, A. and Tobar, M., Design of very high Q sapphire resonators. *Electronics Letters*, 1996, **32**, 670.
5. Klein, N., Zuccaro, C., Daehne, U., Schulz, H., Tellmann, N., Kutzner, R., Zaitsev, A. G. and Woerdenweber, R., Rutile dielectric resonators shielded by YBCO films. *J. Appl. Phys.*, 1996, **78**, 6683–6687.
6. Hao, L. and Gallop, J. C., Spatially resolved measurements of HTS microwave surface impedance. *IEEE Trans. Appl. Supercond.*, 1999, **9**, 1944–1947.
7. Steinhauer, D. E., Vlahacos, C. P., Wellstood, F. C., Anlage, Steven.M., Canedy, C., Ramesh, R., Stanishevsky, A. and Melngailis, J., Imaging of microwave permittivity, tunability, and damage recovery in (Ba, Sr)TiO<sub>3</sub> thin films. *Appl. Phys. Lett.*, 1999, **75**, 3180–3182.
8. Krupka, J., Cros, D., Luiten, A. and Tobar, M., Design of very high Q sapphire resonators. *Electron. Lett.*, 1996, **32**, 670–671.
9. Gallop, J.C. and Hao, L. Applications of coupled dielectric resonators using SrTiO<sub>3</sub> pucks: tuneable resonators and novel thermometry. *IEEE Trans. Instrum. Meas.*, 2001, **50**, 526–530.
10. Lacey, D., Gallop, J. C. and Davis, L. E., The effects of an air gap in the measurement of the dielectric constant of SrTiO<sub>3</sub> at cryogenic temperatures. *Meas. Sci. Technol.*, 1998, **9**, 536–539.
11. Pippard, A. B., *The physics of vibration*. Cambridge University Press, Cambridge, 1978.
12. Gallop, J. C. and Hao, L., Coupled microwave resonators as the basis for sensitive bolometric detection. *IEEE Trans. Instrum. Meas.* (submitted for publication).
13. Hao, L., Gallop, J. C., Klein, N. and Winter, M., Low phase noise temperature—compensated cryogenic whispering gallery mode resonator operated at 63 K in a Closed Cycle Cooler. *IEEE Trans. Instrum. Meas.*, 2001, **50**, 515–518.
14. Abbas, F., Gallop, J. C. and Hao, L., Microwave dielectric composite puck resonators. *Applied Superconductivity (IOP Conference Publication 158)*, 1997, 315–318.